Materials Science-Poland, *Vol. 26*, *No. 2*, *2008*

Synthesis of ceria-based nanopowders suitable for manufacturing solid oxide electrolytes

M. DUDEK*, M. MRÓZ, Ł. ZYCH, E. DROŻDŻ-CIEŚLA

AGH-University of Science and Technology,
Faculty of Materials Science and Ceramics, 30-059 Cracow, Poland

Co-precipitation method and hydrothermal synthesis were used to fabricate nanopowders of pure CeO_2 and singly or co-doped ceria materials in the CeO_2–Sm_2O_3–Y_2O_3 or CeO_2–Gd_2O_3–Sm_2O_3 systems. All sintered powders and samples were found to be pure CeO_2 and ceria-based solid solution of fluorite-type structure. The surface areas of CeO_2-based nanopowders were measured by the one-point BET method. The morphologies of powders were observed by means of transmission electron microscopy. Particle sizes of ceria powders synthesised by the hydrothermal method ranged from 9 to 15 nm, the particle sizes of powders calcined at 800 ºC ranged from 13 to 26 nm. The TEM observations indicated that all CeO_2-based powders consisted of isometric in shape and agglomerated particles. Scanning electron microscope was used to observe the microstructure of the sintered samples. Electrical conductivity was studied by the a.c. impedance spectroscopy in the temperature range 200–700 ºC. The oxygen transference number was determined from EMF measurements of oxide galvanic cells. It was found that co-doped ceria materials such as $Ce_{0.8}Sm_{0.1}Y_{0.1}O_2$ or $Ce_{0.85}Gd_{0.1}Sm_{0.05}O_2$ seem to be more suitable solid electrolytes than singly-doped ceria $Ce_{1-x}M_xO_2$ (M – Sm, Gd, Y, x = 0.15 or 0.20) for electrochemical devices working in the temperature range 600–700 ºC.

Key words: *nanopowder; ceria-based electrolyte; solid oxide fuel cell; electrochemical gas sensor*

1. Introduction

Until now, yttria-stabilized zirconia (8YSZ) is the most often used solid oxide electrolyte in electrochemical devices such as solid oxide fuel cells (SOFC), gas sensors, oxygen pumps and probes for controlling metal processing. This is due to its low electronic and high ionic conductivities, chemical stability under reducing and oxidising atmospheres at high temperatures (800–1000 ºC), moderate mechanical properties and relatively low production costs [1–4]. Lowering of the operation temperature of a SOFC down to around 700–600 ºC would result in an increase in the cell stability

*Corresponding author, e-mail: potoczek@uci.agh.edu.pl

(lower degradation of components) and allow one to use cheaper materials such as ferritic stainless steels for interconnectors [5, 6]. Ceria based solid solutions $Ce_{1-x}M_xO_2$ (Me – Sm, Gd, Y) and x = 0.15–0.20 have been regarded as promising oxide electrolytes for SOFCs and electrochemical sensors for exhaust gases due to higher ionic conductivities than that of fully stabilized zirconia (8YSZ) in the temperature range 600–800 ºC [7, 8]. The main drawback of ceria-based electrolytes, complicating their commercial application, is an increased electronic conduction under low oxygen partial pressure accompanied by reduction of Ce^{4+} to Ce^{3+}[9, 10]. It has been reported that reduction of ceria can be neglected at lower temperatures around 600–700 ºC. However, such low temperatures are not suitable for singly doped ceria as electrolyte in SOFC or other devices, due to high electrical resistance [11]. Structural modification of ceria-based solid solutions by co-doping is one of possible ways to improve their electrical conductivity at this temperature range. Some ternary system involving CeO_2–Sm_2O_3 solid solutions have been studied from viewpoint of structure and electrical properties, the third component being: CaO [12, 13], Y_2O_3 [14], Pr_6O_{11} [15]. Ceria-based materials with the formula depending on chemical composition and phase composition have generally improved electrical conductivity, although in some cases deterioration of the ionic conductivity and increase of electronic conduction is observed. The microstructures of sintered samples, affected by chemical composition, properties of powders and sintering conditions, strongly affect the electrolyte performance [16].

The paper focuses on the preparation of sinterable nanopowders of singly and co-doped ceria materials in the CeO_2–Sm_2O_3–Y_2O_3 or CeO_2–Gd_2O_3–Sm_2O_3 systems as well as on investigation of the properties crucial to application of ceria-based materials as oxide electrolytes in electrochemical devices. The practical aim of this research was to obtain a co-doped ceria based material which could be applied as a component of electrochemical devices working at the temperature range 600–700 ºC.

2. Experimental

The starting materials used in this study were $Ce(NO_3)_3{\times}6H_2O$, $Sm(NO_3)_3{\times}6H_2O$, $Gd(NO_3)_3{\times}6H_2O$ and $Y(NO_3)_3{\times}6H_2O$ (all 99.99% purity, supplied by Aldrich). Aqueous NH_3 solution was used as a precipitating agent. The reagents were mixed in distilled water in order to prepare pure CeO_2, singly doped ceria – $Ce_{1-x}M_xO_2$ (M = Sm, Y, Gd), $0.10 < x < 0.25$ or co-doped ceria-based materials with the formulas $Ce_{0.8}Y_{0.2-x}Sm_xO_2$ or $Ce_{0.85}Gd_{0.15-x}Sm_xO_2$, x = 0.02, 0.05, 0.1, 0.15. A solution containing respective cations was slowly added to continuously stirred NH_3 solution and final pH was adjusted to 10. The co-precipitated products were washed with distilled water. For all compositions, the gels obtained were divided into two parts and used to synthesise ceria-based materials in two different routes. In the co-precipitation-calcination route, (method A), the dried gels were calcined at 800 ºC for 1 h and then rotary-vibratory milled with zirconia grinding media in ethyl alcohol. In

the hydrothermal crystallization route (method B), the gels were hydrothermally treated at 240 ºC for 6 h in water solution under autogeneous water pressure, washed with distilled water and dried at room temperature.

Studies of thermal decomposition processes in the range of 25–1000 ºC, each step 10 ºC /min in air, were conducted using the thermogravimetric analysis (TG), differential thermal analysis (DTA) and evolved gas analysis (EGA) of volatile products with a quadrupole mass spectrometer. The phase compositions of powders and sintered samples were identified using the XRD analysis. X-ray line broadening enabled determination of the sizes of crystallites. Specific surface areas of powders were measured by the one-point BET method. The samples were outgased in vacuum. The results were used to calculate equivalent particle sizes, d_{BET}. The morphologies of powders were observed under transmission electron microscopy. Densification behaviour of pellets was monitored in air via dilatometry using a constant heating rate 5^{o}/min at the 25–1200 ºC temperature range. Scanning electron microscopy observations of the polished and thermally etched surfaces provided quantitative characteristic of the sample microstructures. Apparent density of the sintered bodies was measured by the Archimedean method. To verify stability of materials prepared under reduction conditions, the CeO_2-based samples were isothermally heated at 800 ºC for 24 h in (5 vol. % H_2 in Ar) gas mixture. The fracture toughness K_{Ic} of CeO_2-based samples of polished surfaces was determined by Vickers' indentation. A loading force of 9.81 N imposed for 10 s was applied. The Palmqvist crack model was used [17] to calculate K_{Ic}.

Electrical conductivities were measured by a.c. impedance spectroscopy in the temperature range 200–800 ºC. To estimate the oxygen ion transference number of the ceria-based samples, the EMF of the oxide galvanic cell (1) at the temperature range 500–750 ºC was measured:

$$\mathrm{Pt}|\,\mathrm{O_2}\,(p_1)\;\|\;\text{ceramic oxide electrolyte}\;(\mathrm{O^{2-}})\,\|\mathrm{O_2}\,(p_2)\;|\;\mathrm{Pt} \qquad (1)$$

The electromotive force (EMF) of the cell (1) was measured as a function of temperature (550–700 ºC) and oxygen partial pressure (from 10^{-6} atm to 1 atm). The ionic transference number (t_{ion}) in the sample was calculated based on the electromotive force (EMF) values (E_m) measured for the cell (1) and on the EMF values (E_t) obtained for the cell (1) with a pure oxygen ion conductor. The procedure was similar to that described in Ref. [12].

3. Results and discussion

Typical DTA and TG curves recorded for samaria-doped ceria $Ce_{0.85}Sm_{0.15}O_2$ (15SDC) precursor, obtained by the method A are shown in Fig 1. First feature seen on the DTA curve at ~100 ºC is an endothermic peak connected with dehydration and a significant loss in weight. Following the dehydration, the continuous heating causes decomposition of NH_4NO_3 and other nitrate precursors leading also to a large weight

loss at temperature range 100–500 ºC. An exothermic peak at ~ 270 ºC probably originated from crystallisation of ceria solid solution. The observations were confirmed by the EGA measurements. They also revealed that both decomposition of nitrates and crystallisation of ceria solid solution proceeded with formation of NO, NO_2, N_2O, O_2 and H_2O. Above 500 ºC, the sample weight remained unchanged, indicating that a stable crystalline CeO_2 structure formed.

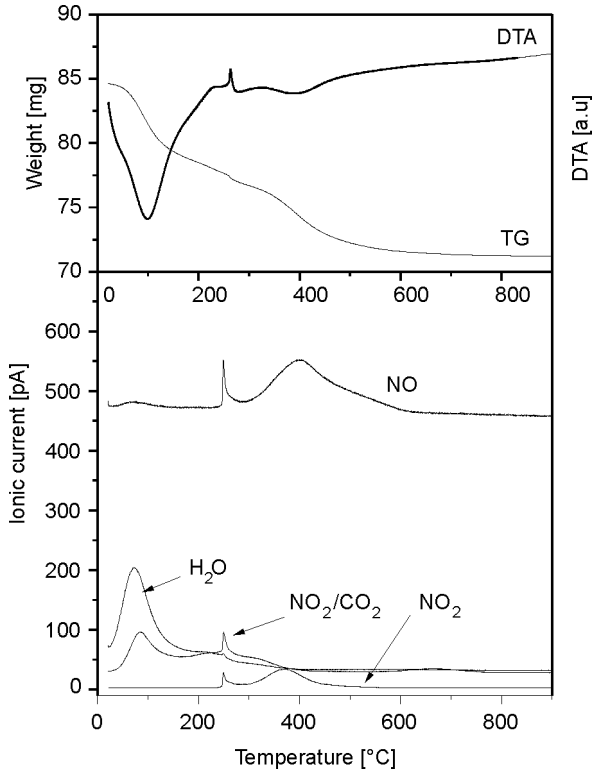

Fig. 1. DTA, TG and EGA curves of the $Ce_{0.85}Sm_{0.15}O_2$ (15SDC) dried precursor obtained by the co-precipitation-calcination method

Figure 2 shows XRD patterns of the $Ce_{0.85}Sm_{0.15}O_2$ (15SDC) dried (a) precursor and its calcination product at 290 ºC (b), 500 ºC (c) and 800 ºC (d) The XRD pattern of $Ce_{0.85}Sm_{0.15}O_2$ sintered sample (e) is also given. The XRD pattern recorded for 15SDC dry sample reflects CeO_2 structure but the peaks are wide and their intensities low. It appears from Fig. 2 that with increasing temperature the half-widths of peaks become lower and their intensities stronger. Fully crystalline patterns of $Ce_{0.85}Sm_{0.15}O_2$ solid solutions were observed at temperatures above 600 ºC. Similar DTA, TG curves and XRD patterns were recorded for other chemical compositions of singly or co-doped ceria samples.

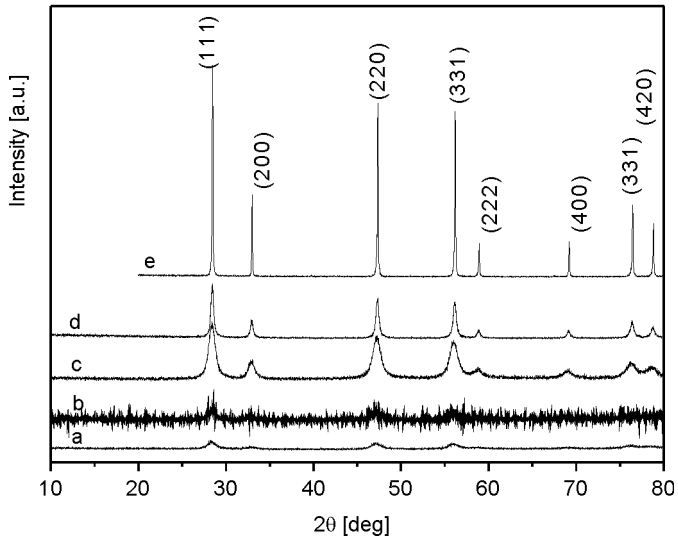

Fig. 2. Evolution of the XRD diffraction patterns recorded for the 15SDC dried precursor (a) and after calcination at 290 ºC (b), 700 ºC (c) and for sample sintered at 1500 ºC for 2 h (d)

Only CeO_2 phase was identified by the XRD analysis in all powders obtained by the methods A and B and also in the sintered samples. No phases other than cubic CeO_2 were found in the XRD diffraction patterns of the samples exposed in an (H_2–Ar) gas mixture. Basic characteristics of the starting powders obtained by both methods are collected in Table 1. The data show that crystallite sizes of hydrothermally synthesised CeO_2-based powders ranged from 7 nm to 16 nm. The CeO_2-based powders with the same chemical composition but calcined at 800 ºC, consisted of larger particles (17–29 nm in size).

Table 1. Basic data on pure CeO_2, and co-doped ceria based powders obtained by co-precipitation calcination (A) method and hydrothermal (B) synthesis

Parameter	CeO_2	$Ce_{0.8}Sm_{0.2}O_2$ (20SDC)	$Ce_{0.8}Y_{0.1}Sm_{0.1}O_2$ (10S10YDC)	$Ce_{0.85}Gd_{0.15}O_2$ (15GDC)	$Ce_{0.85}Gd_{0.1}Sm_{0.05}O_2$ (10G5SDC)
Crystallite size, $d_{(hkl)}$ [nm]	17.4 (A) 6.2 (B)	24.8 (A) 14.6 (B)	23.2 (A) 14.1 (B)	24.8 (A) 12.8 (B)	25.7 (A) 14.6 (B)
Particle size, $d_{(BET)}$ [nm]	29.4 (A) 11.2 (B)	36.5 (A) 21.4 (B)	34.4 (A) 24.4 (B)	32.1 (A) 19.4 (B)	40.2 (A) 22. 2 (B)

The consistency of particle sizes determined by the X-ray analysis and BET surface measurements suggest that the powders are mostly composed of isometric and rather weakly agglomerated particles. A small increase of particle size (Fig. 3) was observed with samarium $Ce_{1-x}M_xO_2$, $Ce_{0.8}Y_{0.2-x}Sm_xO_2$ or $Ce_{0.85}Gd_{0.15-x}Sm_xO_2$ solid solutions compared to pure CeO_2. The TEM observations of 15SDC powder calcined at 800 ºC for 1h (Fig. 4a) or crystallized in water solution under autogeneous water

pressure (240 ºC, 6 h) (Fig. 4b) revealed presence of agglomerated particles of 15SDC powders and confirmed conclusions derived from X-ray and BET examinations.

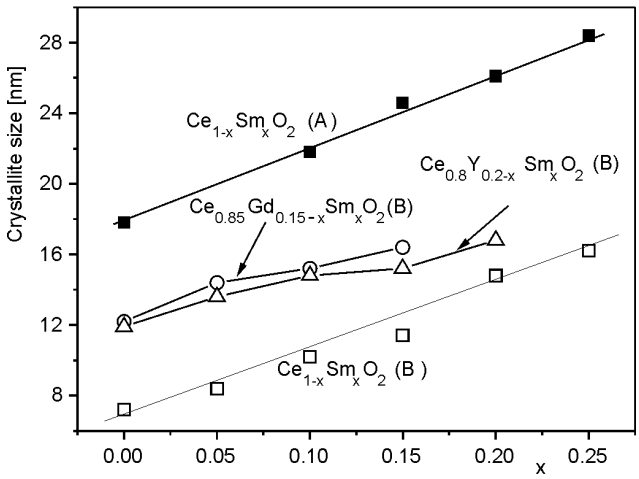

Fig. 3. Dependence of crystallite size on samarium content x in singly doped ceria $Ce_{1-x}Sm_xO_2$ and co-doped ceria $Ce_{0.8}Y_{0.2-x}Sm_xO_2$ or $Ce_{0.85}Gd_{0.15-x}Sm_xO_2$ powders obtained by the co-precipitation calcination metod (A) and hydrothermal synthesis (B)

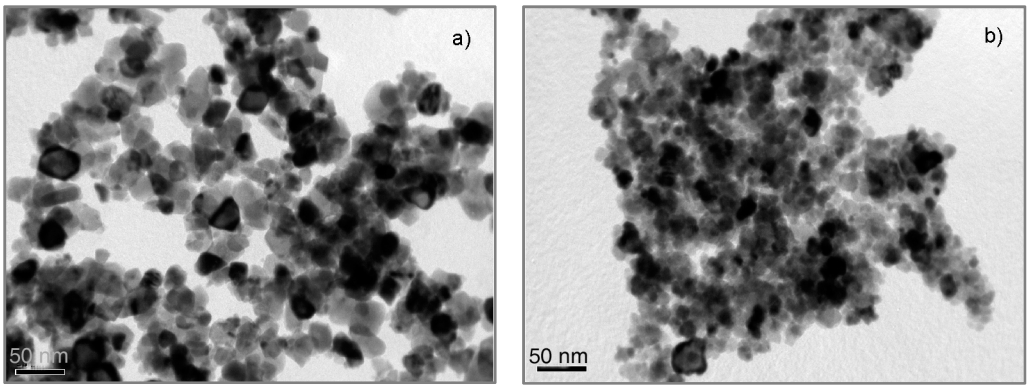

Fig. 4. TEM micrographs of 15SDC powders obtained from:
a) co-precipitation calcination method, b) hydrothermal treatment of co-precipitated gel

Further observations of all powders allow us to state that there are no distinct differences in their morphologies, irrespective of the rate of their fabrication. Figure 5 shows the densification of selected pellets obtained from the investigated powders. For all pellets the shrinkage began at 200 ºC and on further heating an intensive densification started at ca. 450–500 ºC or 800–1000 ºC for samples obtained from powders synthesized by hydrothermal (B) or co-precipitation calcination (A) method, respectively.

Hydrothermally synthesised ceria-based materials sintered at 1300–1350 ºC for 2 h exhibited relative densities higher than 98%. On the other hand, CeO_2-based solid

solutions with formula $Ce_{1-x}Sm_xO_2$, Me – Sm, Gd, Y, $0 < x < 0.25$ or co-doped ceria materials $Ce_{0.8}Y_{0.2-x}Sm_xO_2$, had to be sintered at 1500–1550 ºC for 2 h to obtain more than 96% of theoretical densities. Figure 6 shows the microstructure of $Ce_{0.8}Sm_{0.1}Y_{0.1}O_2$ samples sintered at 1500 ºC or 1350 ºC for 2 h. Both samples were characterized by isometric grains of 0.3–0.6 μm (method B) or 3–5 μm (method A) in size. No additional cracks and pores were observed for co-doped ceria samples after additional hydrogen treatments. The obtained results indicate that the investigated methods are suitable for preparation of fine sinterable powders for manufacturing gas tight samples which could be applied as solid electrolytes in electrochemical devices.

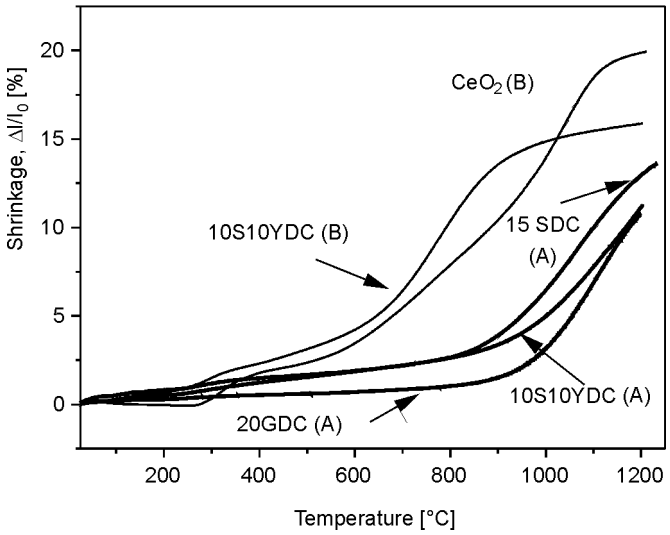

Fig. 5. Dilatometric curves recorded for selected CeO_2-based pellets obtained from powders prepared by co-precipitation-calcination method (A) and hydrothermal synthesis (B)

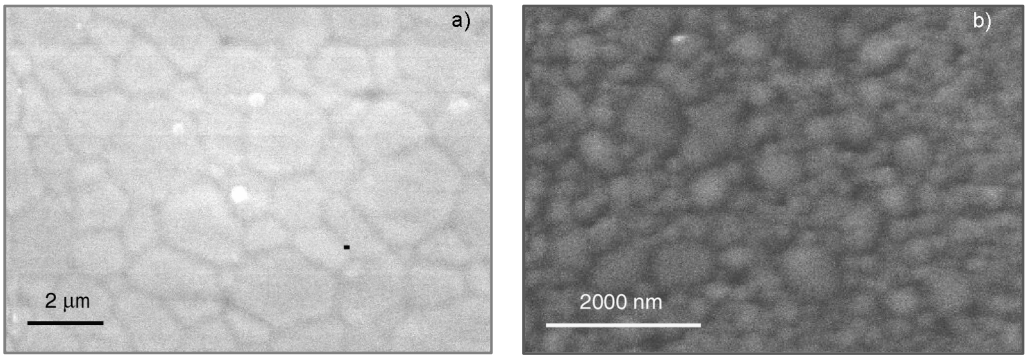

Fig. 6. Microstructures of $Ce_{0.8}Sm_{0.1}Y_{0.1}O_2$ ceramics obtained from powders synthesised by the method A, sintered at: 1500 ºC for 2 h (a), and by the method B, sintered at 1350 ºC for 2 h (b)

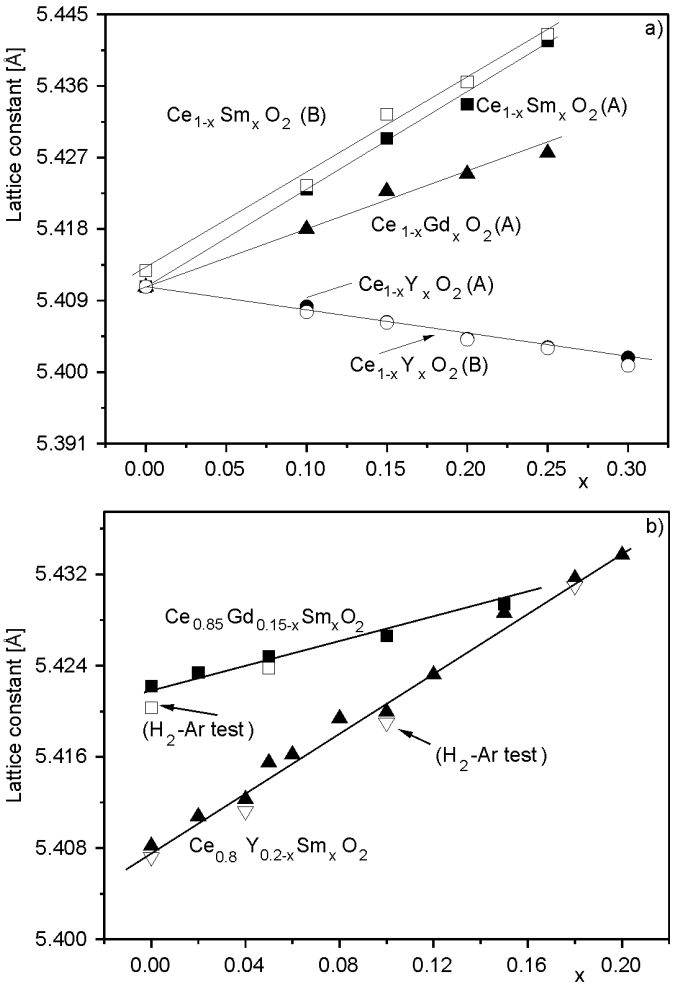

Fig. 7. The lattice constant of singly doped ceria $Ce_{1-x}Me_xO_2$ (Me – Sm, Gd, Y) (a) and $Ce_{0.8}Y_{0.2-x}Sm_xO_2$ or $Ce_{0.85}Gd_{0.15-x}Sm_xO_2$ (b) obtained from powders synthesised by co-precipitation calcination method (A) and hydrothermal synthesis (B); samples sintered at 1500 ºC or 1350 ºC for 2 h

The lattice parameters of $Ce_{1-x}M_xO_2$, M – Sm, Gd, $0 < x < 0.25$ and co-doped ceria-based materials $Ce_{0.85}Gd_{0.85-x}Sm_xO_2$, or $Ce_{0.8}Y_{0.2-x}Sm_xO_2$ (Fig. 7) linearly increased with x but the slope was lower for ceria samples doubly doped with gadolinium and samarium than for those doped with yttrium and samarium. The decrease of the lattice parameter is observed for ceria–yttria solid solution. These observations are in good agreement with effective ionic radius considerations [18]. An additional heat treatment in 10 vol. % H_2–Ar gas mixtures caused a small decrease of cell parameters of all investigated samples.

Good mechanical properties of CeO_2-based ceramics are also necessary for applications as solid electrolytes in SOFCs, sensors for exhaust gases in automotive indus-

try. The fracture toughness K_{Ic} (Table 2) measurements for selected samples revealed a small increase in the fracture toughness with increasing samarium, gadolinium or yttrium content in $Ce_{1-x}M_xO_2$ compared to pure CeO_2. On the other hand, in the case of co-doped ceria materials with the formula $Ce_{0.8}Sm_{0.2-x}Y_xO_2$ or $Ce_{0.85}Gd_{0.15-x}Sm_xO_2$, $0 < x < 0.15$, the fracture toughness remains unchanged within an experimental error. The values of K_{Ic} for 8YSZ samples are also presented in Table 2. The results given in the table indicate that ceria based materials have slightly worse mechanical properties than the 8YSZ electrolyte.

Table 2. Fracture toughness K_{Ic} determined for CeO_2-based materials

Material	D, average grain size [μm]	K_{Ic} MPa×m$^{0.5}$
CeO_2	11.51 (A)	1.3± 0.2
$Ce_{0.85}Sm_{0.15}O_2$	3.89 (A)	2.1± 0.2
	0.58 (B)	2.4 ±0.1
$Ce_{0.8}Sm_{0.2}O_2$	3.41 (A)	2.2± 0.2
	0.48 (B)	2.3±0.1
$Ce_{0.85}Gd_{0.15}O_2$	3.16 (A)	1.9±0.1
	0.54 (B)	2.1±0.2
$Ce_{0.8}Y_{0.2}O_2$	2.80 (A)	1.7±0.3
	0.62 (B)	1.9±0.2
$Ce_{0.8}Sm_{0.1}Y_{0.1}O_2$	2.68 (A)	2.2± 0.3
	0.67 (B)	2.4± 0.2
$Ce_{0.85}Gd_{0.1}Sm_{0.05}O_2$	3.12 (A)	2.1±0.3
	0.56 (B)	1.9±0.2
8YSZ	2.68 (A)	2.8 ± 0.2
	0.55 (B)	3.2± 0.2

Table 3. Electrical conductivities σ at 600 ºC of the CeO_2-based samples obtained from powders prepared the co-precipitation calcination (A) or hydrothermal method (B)

Composition	σ [S/cm]		E_a [eV]	
	Bulk	Grain boundary	Bulk	Grain boundary
CeO_2	6.16×10^{-5}	1.21×10^{-6}	1.51	1.81
$Ce_{0.85}Sm_{0.15}O_2$	5.72×10^{-3} (A)	4.23×10^{-3} (A)	0.84	1.01
	1.56×10^{-2} (B)	1.34×10^{-2} (B)	0.82	0.89
$Ce_{0.8}Sm_{0.2}O_2$	6.61×10^{-3} (A)	5.18×10^{-3} (A)	0.87	0.98
	1.11×10^{-2} (B)	1.89×10^{-2} (B)	0.80	0.88
$Ce_{0.8}Y_{0.2}O_2$	4.68×10^{-3} (A)	1.18×10^{-3} (A)	0.98	1.06
	9.47×10^{-3} (B)	5.53×10^{-3} (B)	0.93	0.97
$Ce_{0.8}Sm_{0.1}Y_{0.1}O_2$	8.16×10^{-3} (A)	7.62×10^{-3} (A)	0.82	0.93
	2.06×10^{-2} (B)	2.56×10^{-2} (B)	0.78	0.84
$Ce_{0.85}Gd_{0.15}O_2$	6.87×10^{-3} (A)	5.17×10^{-3} (A)	0.93	1.04
	1.16×10^{-2} (B)	1.14×10^{-2} (B)	0.89	0.96
$Ce_{0.85}Gd_{0.1}Sm_{0.5}O_2$	8.15×10^{-3} (A)	7.86×10^{-3} (A)	0.92	1.01
	2.67×10^{-2} (B)	1.62×10^{-2} (B)	0.85	0.92

Impedance spectroscopy measurements enabled one to determine the bulk (σ_b) and grain boundary (σ_{gb}) conductivities of CeO_2-based samples. Respective values of the conductivities at 600 ºC are given in Table 3. The values of activation energy calculated for the temperature range 200–800 ºC are also given. It can be seen from Table 3 that the bulk and grain boundary conductivities of $Ce_{1-x}M_xO_2$, M – Sm, Y, Gd increased up to x = (0.15–0.20) and decreased for higher substitution levels. The activation energy shows an opposite trend. As previously reported [19], ionic conductivities are significantly enhanced in $Ce_{1-x}Sm_xO_2$ solid solutions by increasing the concentration of oxygen vacancies ($V_O^{\bullet\bullet}$), ascribed to defect associations of the type $Sm'_{Ce}V_O^{\bullet\bullet}$ at higher concentrations of x. The introduction of yttria into ceria–samaria solid solutions caused a small increase of ionic conductivity. The total electrical conductivity (calculated as a sum of grain boundary and bulk conductivities) reached a maximum value of 1.60×10^{-2} or 4.58×10^{-2} (S/cm) at 600 ºC for $Ce_{0.8}Sm_{0.1}Y_{0.1}O_2$ sintered samples obtained by the methods A or B, respectively. A partial substitution of gadolina by samaria in $Ce_{0.85}Gd_{0.15-x}Sm_xO_2$ up to x = 0.05 also improves the total electrical conductivity compared to only ceria-doped gadolina $Ce_{0.85}Gd_{0.15}O_2$.

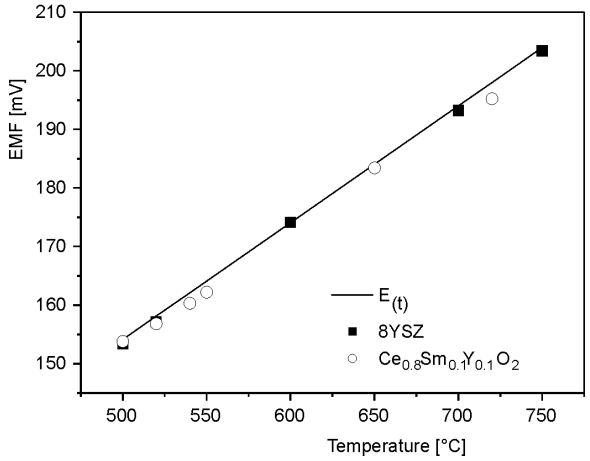

Fig. 8. Temperature dependence of the EMF of cell (1); working electrode – Pt | (Ar–O_2) p_2 =2×10^{-5} atm, reference electrode – Pt | air

The EMF values of the cell (1) measured in the temperature range 500–750 ºC (Fig. 8) were compared with the EMF (E_t) values obtained for the cell containing 8YSZ. The calculated values of the transference oxygen numbers (t_{ion}) for $Ce_{0.8}Me_{0.2}O_2$ or $Ce_{0.85}Me_{0.15}O_2$, Me – Sm, Gd, Y, and for co-doped ceria based samples $Ce_{0.8}Y_{0.1}Sm_{0.1}O_2$ or $Ce_{0.85}Gd_{0.1}Sm_{0.05}O_2$ were close to 1, which indicates practically pure oxygen ionic conductivity in the investigated samples. A comparison of the changes of electrical conductivities of ceria-based solid solutions indicates that the reason of the conductivity enhancement with respect to singly-doped ceria is an increase in concentration of oxygen vacancies.

4. Conclusions

Singly-doped ceria or co-doped ceria materials CeO_2–Sm_2O_3–Y_2O_3 or CeO_2 –Gd_2O_3–Sm_2O_3 were successfully prepared both from powders obtained by the co-precipitation calcination (A) method and hydrothermal (B) synthesis. The application of ceria-based powders prepared by the hydrothermal synthesis allowed one to reduce the sintering temperature of ceria based electrolytes from 1500 ºC to ca. 1300–1350 ºC. Higher sintering temperatures lead to high manufacturing costs for SOFC systems because ceria based electrolytes and other components such as cathode and anode cannot be cofired at higher temperatures (e.g. higher than 1300 ºC). Contrary to mechanical properties, the electrical conductivity of ceria-based electrolytes can be improved by controlling the grain sizes. The obtained values of electrical conductivities and activation energies for $Ce_{0.8}Sm_{0.1}Y_{0.1}O_2$ or $Ce_{0.85}Sm_{0.1}Gd_{0.05}O_2$ with average grain size of 0.5–0.7μm show that the prepared materials seem to be promising materials for SOFCs and other electrochemical devices operating at 600–700 ºC.

Acknowledgement

This work was carried out under contracts no 3T08 D01926 (2004–2007) with the Polish Scientific Research Committee.

References

[1] FERGUS J.W., J. Power Sources, 162 (2006), 30.
[2] MINH N.Q., TAKAHASHI T., *Science and Technology of Ceramic Fuel Cells*, Elsevier, Amsterdam 1995.
[3] GIBBSON R.W., KUMAR R.V., FRAY D.J., Solid State Ionics, 121(1999), 43.
[4] BESRA L., COMPSON CH., LIU M., J. Am. Ceram. Soc., 89 (2006), 3003.
[5] TIETZ F., BUCHKREMER H., STÖVER., Solid State Ionics, 152–153 (2002), 373.
[6] BRYLEWSKI T., NANKO M., MARUYAMA T., PRZYBYLSKI K., Solid State Ionics, 143 (2001), 131.
[7] INABA H., TAGAWA H., Solid State Ionics, 83 (1996), 1.
[8] KHARTON V., FIGUEIREDO F., NAVARRO L., NAUMOVICH E., KOVALEVSKY A., YAREMCHENKO A., VISKUP A., CARNEIRO A., MARGUES M., FRADE J., J. Mater. Sci., 36 (2001),1105.
[9] XIONG Y., YAMAJI K., HORITA T., SAKAI N., YOKOKAWA H., J. Electrochem. Soc., 149 (2002), 450.
[10] SAMESHIMA S., HIRATA Y., EHIRA Y., J. All. Comp., 408–412(2006),628.
[11] HONG J., MEHTA K., J. Electrochem. Soc., 145 (1998), 638.
[12] MORI T., IKEGAMI T., YAMAMURA H., J. Electrochem. Soc., 146 (1999), 4380.
[13] DUDEK M., ZIEWIEC K., Adv. Mater. Sci., 6 (2006), 53.
[14] SHA X., LÜ Z., HUANG X., MIAO Z., JIA L., XIN X., SU W., J. All. Comp., 424 (2006), 315.
[15] JI Y., LIU J., HE T., WANG J., SU W., J. All. Comp., 389 (2005), 317.
[16] DRENNAN J., AUCHTERLONIE G., Solid State Ionics, 134 (2000), 75.
[17] NIIHARA K.., J. Mater. Sci. Lett., 2 (1983), 221.
[18] SHANNON R., PREWITT T., Acta Cryst. B, 25 (1969), 925.
[19] HUNG W., SHUK P., GREENBLATT M., Solid State Ionics, 113–115 (1998), 305.

Received 28 April 2007
Revised 16 February 2008